Case Studies in Engineering Failure Analysis 5–6 (2016) 51–58

Contents lists available at ScienceDirect

Case Studies in Engineering Failure Analysis

journal homepage: www.elsevier.com/locate/csefa

Case study

Research on the failure of the induced draft fan's shaft in a power boiler

Jinfeng Du *, Jun Liang, Lei Zhang

Center of Technology Research, Shenhua Guohua Electric Power Research Institute Co., Ltd, Beijing 100025, PR China

ARTICLE INFO

Article history:
Received 5 November 2015
Received in revised form 26 January 2016
Accepted 8 February 2016
Available online 15 February 2016

Keywords:
Torsional vibration
Stress concentration
Network pearlite
Fracture
Ratchet-like characteristic

ABSTRACT

The failure of the induced draft fan's shaft in a power boiler was been analyzed. The performances of material applied satisfied the design requirement. The order torsional vibration showed anomaly at the shaft's smallest diameter for the design condition and the actual radius of that chamfer less than the design radius caused more significant stress concentration. The additive effect of the abnormal torsional vibration and the higher stress concentration induced the microcrack's initiation along the network pearlite's interface. The vibration and the alternating torsional loading in the induced draft fan's service led to crack growing along the different direction and fracture presenting the typical ratchet-like characteristic.

1. Introduction

Now the frequency conversion driving technology had been applied widely to adjust the running load of boiler fan in order to improve the unit's efficiency for it was beneficial to reducing the energy consumption of the firepower plant [1–5]. With the increase in the fan's parameters and the application of the frequency changer, the torsional resonance easily occurred for the shaft which connected the boiler fan with the frequency changer when the boiler fan was in the variable speed operation. Once the torsional resonance appeared and was not eliminated timely, the shaft's failure would not be avoided [6–9].

The induced draft fan of a power plant in 2012 suddenly appeared the abnormal phenomenon when it was running in condition of the variable frequency. The shaft of the induced draft fan was found to fracture after the emergency shutdown and the fracture happened near the site of the shaft's variable diameter. The shaft's smallest diameter was 225 mm and the chamfer of the shaft shoulder is less than 2 mm, as shown in Fig. 1. In this paper, the failure investigation had been paid attention to the analysis of failure cases which ranged from material performance, equipment's design to service condition of equipment, and thus the preventive measures were developed in order to avoid the recurrence of the similar failure.

2. Experiment

The experimental work consisted of two parts: the first covered the analysis of the failed shaft's performance and fracture; the second included the analysis of the stress, the torsional resonance and the shaft's design.

* Corresponding author. Tel.: +86 10 8595 7107.
E-mail address: dujinfenghqf@126.com (J. Du).

http://dx.doi.org/10.1016/j.csefa.2016.02.002

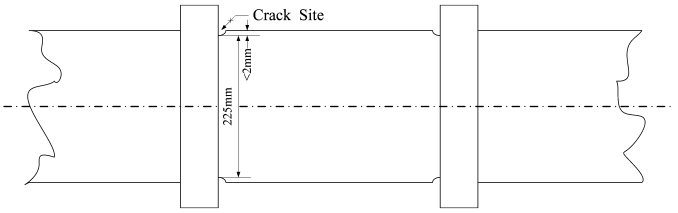

Fig. 1. The schematic diagram of the cracking location on the shaft.

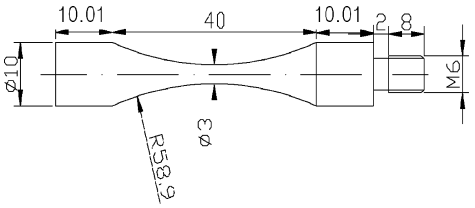

Fig. 2. The specimen of ultrasonic fatigue.

2.1. Analysis of the failed material

The failed material component was analyzed firstly by Delta DP2000. The analysis of specimens' microhardness was carried out through FM-700 with the load of 9.8 N and the hold time of 14 s. The tensile test was conducted using MTS-880 machine at the constant loading rate of 2 mm/min in the room temperature. The fatigue test was carried out through USF-2000 and the experimental frequency was 20 kHz. The experimental temperature changes 25–35 °C and the experimental humidity changes 40–60%. Fatigue test was carried under the different stress and load ratio $R = -1$. The cycle time changed from 10^3 to 10^8. The ultrasonic fatigue specimen was shown in Fig. 2.

Specimens were taken from the fracture to carry out the metallurgical analysis and the SEM analysis, as shown in Fig. 3. The part A was used for the metallurgical analysis and the part B was used for the SEM analysis.

2.2. Analysis of stress distribution, torsional resonance and the shaft structure

Based on the finite element method and the lumped mass method, the analysis of the stress distribution and torsional resonance were carried out. Compared the actual structure with the design structure, the effect of the manufacturing process on the shaft's life was investigated.

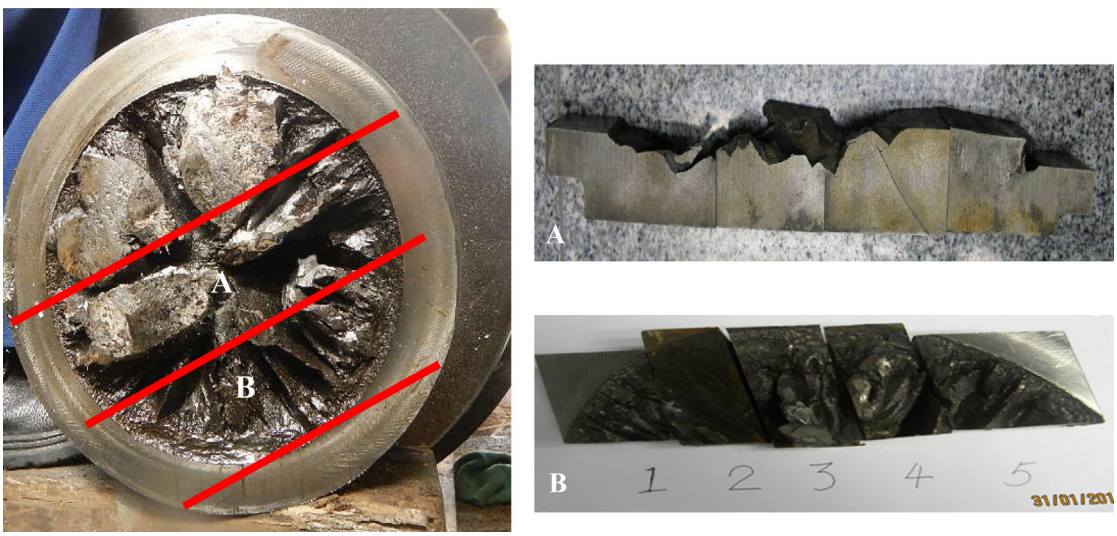

Fig. 3. The samples for metallographic and SEM analysis.

3. Result analysis

3.1. Analysis of the shaft's mechanical performance

According to the design requirement, the material applied should be Q345B.

Table 1 showed the failed material's chemical composition and National standard [10], the comparing result indicated the applied material's chemical composition accorded with the corresponding National standard. Thus the material's selection complied with the design requirement from the perspective of chemical composition.

Fig. 4 showed the microhardness, yield strength and tensile strength of the failed material. The average of microhardness, yield strength and tensile strength were about 157 HV, 349 MPa and 527 MPa respectively, which showed the material property met the corresponding National standard [10]. That proved the material applied was good at the quality and the shaft failure was not relate to the material property.

The S–N curve of Q345B based on the ultrasonic fatigue experiment was shown in Fig. 5. With the reduction of the stress level, the fatigue life increased gradually. But the cyclic time was always higher than 10^6 when the stress amplitude was lower than the shaft's fatigue strength (σ_{-1}) which was about 265 MPa. It was close to the value (269 MPa) which was calculated by following the equation [11]

$$\sigma_{-1} = 0.285(\sigma_s + \sigma_b) \tag{1}$$

where σ_s was the yield strength, σ_b was the tensile strength.

Ideally, there was a relationship between the torsional fatigue strength (τ_{-1}) and the fatigue strength (σ_{-1}), as shown in the equation [11]

$$\tau_{-1} = 0.5\sigma_{-1} \tag{2}$$

However the effect of several factors on the torsional fatigue strength needed to be taken into account after material had been processed to the shaft, for example the factor of the shaft's size, load fluctuation of the shaft, processing quality coefficient of the shaft, the shaft's service condition and the effective stress concentration factor. Thus the shaft's torsional fatigue strength (τ^*_{-1}) had been revised by following the equation [11]

$$\tau^*_{-1} = \tau_{-1} \times \frac{\epsilon_\tau \beta}{\tau} \tag{3}$$

Table 1
Comparison of chemical composition of studied material and National standard [10].

Element (wt. %)	C	Si	Mn	P	S	Cu	Ni	Cr	Mo	V
Specimen	0.18	0.44	1.36	0.017	0.007	0.226	0.069	0.108	0.023	0.008
National standard	≤0.20	≤0.50	≤1.7	≤0.04	≤0.04	≤0.30	≤0.012	≤0.30	≤0.10	≤0.15

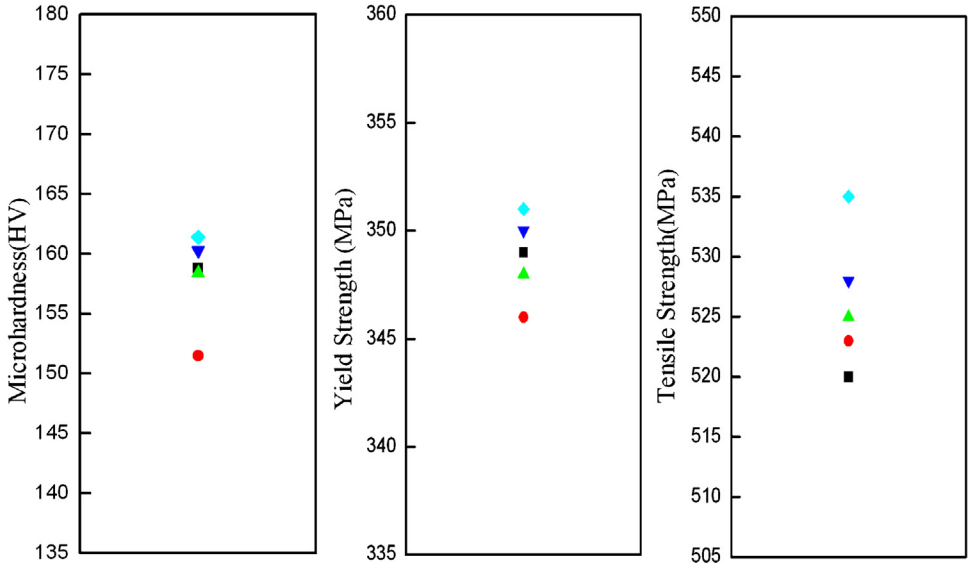

Fig. 4. The mechanical property of the applied material.

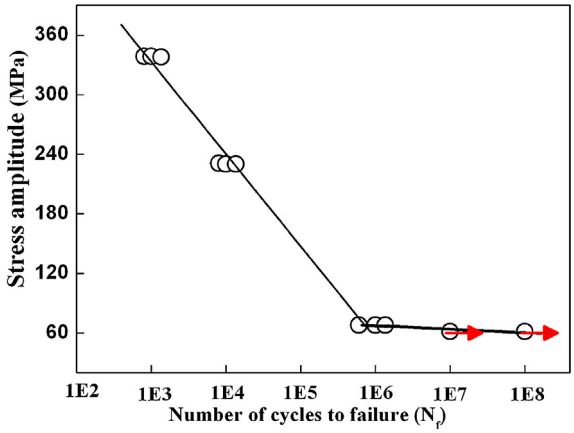

Fig. 5. The applied material's S–N curves based on the ultrasonic fatigue.

where ε_τ was the factor of the shaft's size, β was the coefficient of processing quality, τ was the effective stress concentration factor. Combined Eqs. (2) and (3), the revised τ^*_{-1} was 54.15 MPa when the σ_{-1} was 265 MPa; ε_τ was 0.99, β was 0.9 and τ was 2.18 which were supplied by the shaft's design institute.

3.2. Analysis of the shaft's fracture

Fig. 6 showed the macroscopic feature of the shaft's fracture. From Fig. 6(a), the fracture was scraggly and it was more than 40 mm between the highest site and the lowest site for the fracture by means of the stereo microscope. So it was the

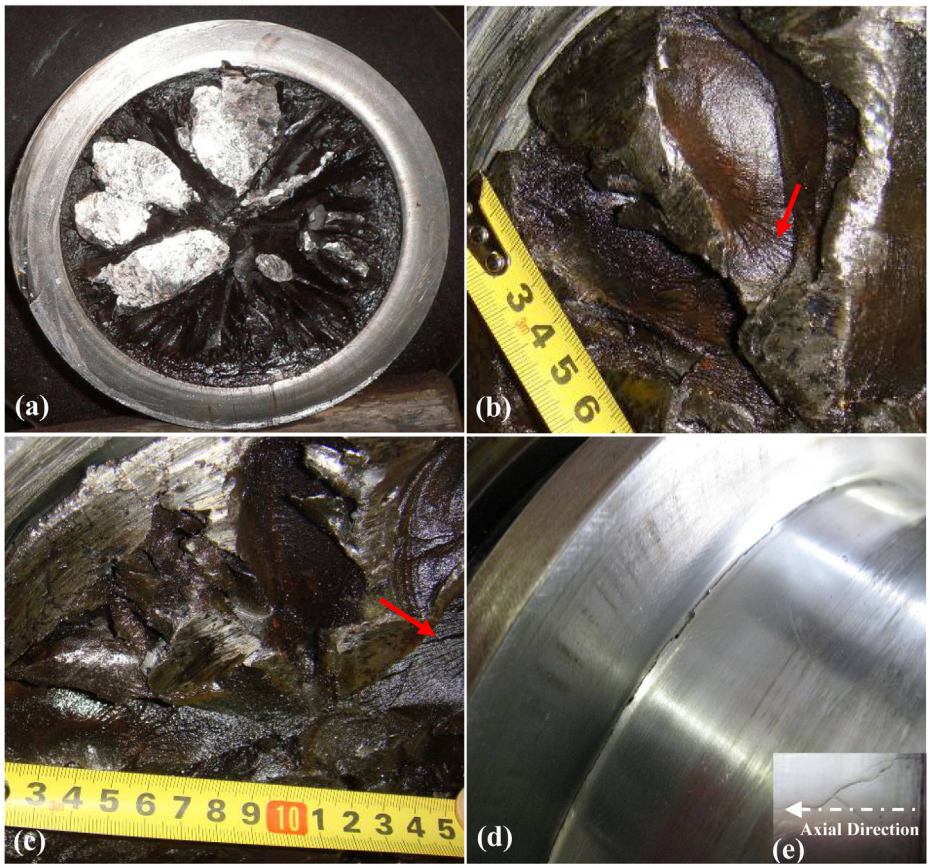

Fig. 6. The macroscopic feature of the shaft's fracture (a) whole facture morphology; (b) beach marks; (c) fatigue cracks; (d) location of crack; (e) direction of crack growing.

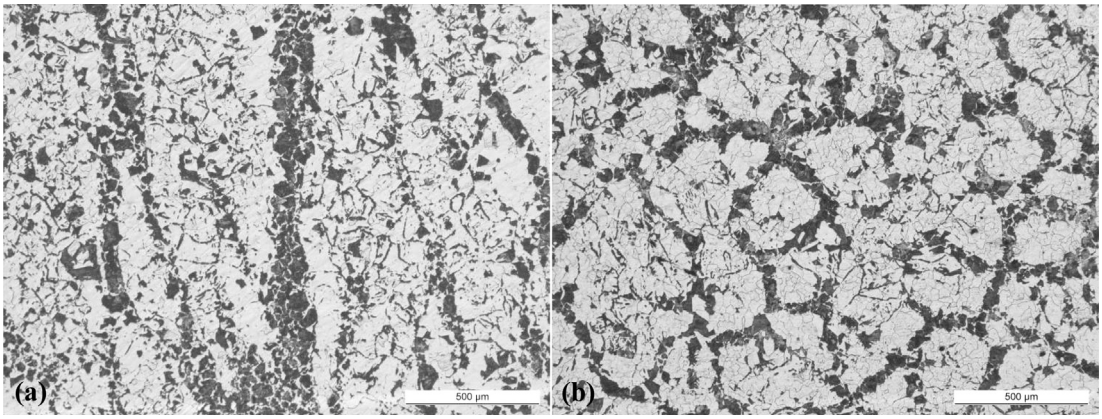

Fig. 7. The microstructure of the fracture's different section (a) band-pearlites at the vertical section (b) network-pearlites at the cross section.

typical morphology of the ratchet-like fracture. Some beach marks and fatigue cracks were observed, as shown in Fig. 6(b) and (c). Fig. 6(d) showed the cracks on the surface of other shaft which was same to the failed shaft from the view of material selection and service condition. Some cracks appeared at the surface of the shaft's shoulder chamfering and the crack grew along an angle of 45° to the axial direction, as shown in Fig. 6(e). It was confirmed that this shaft having cracks would fracture if it continued to work and the fractured position was also in the site of the minimum diameter.

Fig. 7 showed the microstructure of the fracture's different section. The microstructure of material was ferrite and pearlite. The massive lamellar pearlites presented the obvious zonal distribution from the vertical section; the slender strip's pearlite showed the reticular distribution from the cross section and distributed along the ferrite grain boundaries. According to the National standard [12], the banded structure was evaluated as the degree 4. Although material mechanical

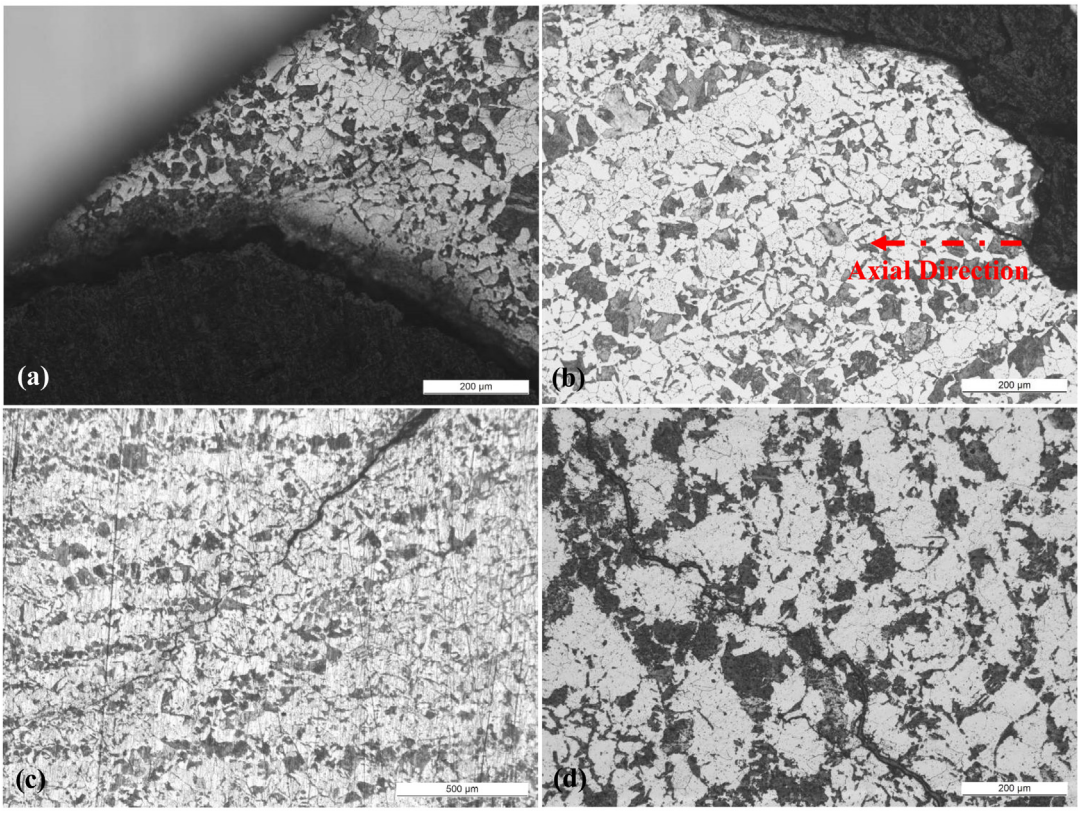

Fig. 8. The crack's initiation and propagation (a) the crack at the chamfer, (b) the secondary crack, (c) the crack's propagation (the longitudinal section), and (d) the crack's propagation (the cross section).

properties were good, the networked-like pearlite structures might affect the material's applying performance once it served under the improper operational condition.

The crack's initiation and growth at the different section of the unfractured shaft were shown in Fig. 8. The crack initiated from the edge of the chamfer and grew along an angle of 45° to the axial direction. From Fig. 8(c) and (d), it was found that crack grew along the interface of the ferrite and the pearlite. So the interface was the weak position, the trend was intensified especially when the network pearlite had formed at the ferrite's boundaries.

Fig. 9 showed the SEM images of the shaft's fracture. Most of fracture surface morphology were some torn edges, river pattern and small cleavage facets, so it confirmed the shaft's fracture was brittle fracture and the fracture showed the typical quasi-cleavage characteristic. The some secondary cracks appeared at the torn edge's bottom and the shallow dimple, and they was taken as the microcrack's source; some microcracks got together to form the crack, and the crack growth resulted in fracture. A large number of the multi-direction fatigue cracks were observed on the fracture's surface, and it was confirmed that the shaft underwent the fatigue damage which was caused by the vibration.

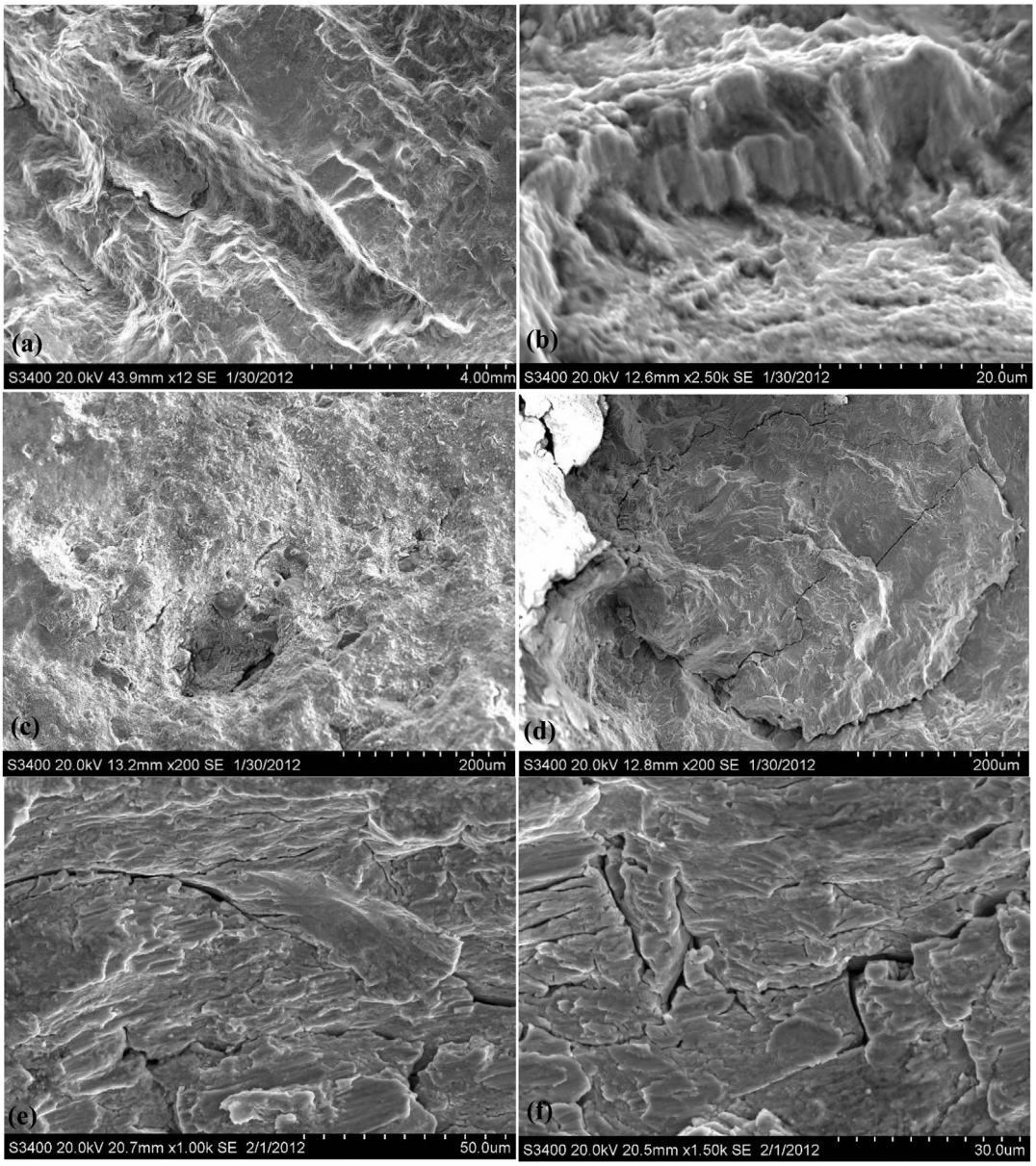

Fig. 9. The SEM images of the fracture (a) the torn edge, (b) the end of torn edge, (c) the shallow dimple, (d) the secondary crack around the shallow dimple, (e) the river pattern and (f) the fatigue crack.

3.3. Analysis of the stress and torsional vibration

The shaft's solid model and the shaft's calculation model based on the finite element method were shown respectively in Fig. 10(a) and (b). The shaft's stress distribution obtained which is based on the induced draft fan's rated torque (58625 N m) was presented in Fig. 10(c), the stress concentration was significant at the site of the shaft shoulder's chamfer. The maximum shear stress (τ_{max}) obtained by the ANSYS simulation was 63 MPa. The maximum allowable shear stress (τ_n) was obtained by the equation [11]

$$\tau_n = \frac{T}{\pi d^3/16} \tag{4}$$

where T was the rated torque (58625 N m), d was the smallest diameter of shaft's chamfer (225 mm), τ_n was the maximum allowable shear stress and τ_n was 26.3 MPa.

The stress concentration factor (k) was obtained by the equation [11]

$$k = \frac{\tau_{max}}{\tau_n} \tag{5}$$

where τ_{max} was the maximum shear stress, τ_n was the nominal maximum shear stress. Then k was 2.4 at the site of the shaft's variable diameter, and it was in a relatively high level. So this also proved that there existed the more significant stress concentration. Therefore the occurrence of fatigue failure at the shaft's variable diameter was earlier than other position.

The shaft's three-dimensional model was built based on the design size, as shown in Fig. 11(a). The result calculated with applying the lumped mass method showed that the order torsional vibration was anomalous at the shaft's smallest diameter when the shaft was in the critical speed (920 rpm), and the torsional stress was maximal at the smallest diameter.

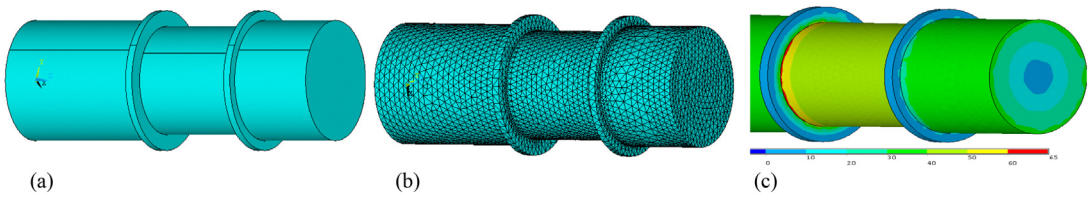

Fig. 10. The shaft's solid model and the shaft's calculation model based on the finite element method (a) solid model, (b) calculation model, and (c) stress distribution.

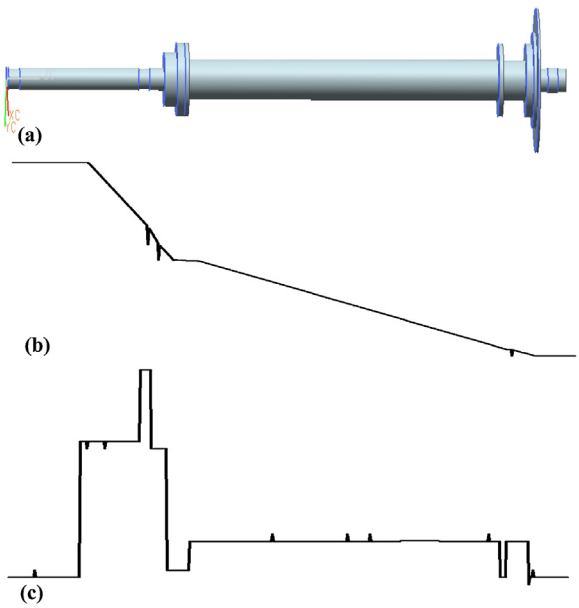

Fig. 11. The shaft's three-dimensional model and the order torsional vibration's mode and the torsional stress distribution (a) the three-dimensional model, (b) the order torsional vibration's mode, and (c) the torsional stress distribution.

4. Discussion

Based on the shaft's design size, the result of the finite element simulation showed that the stress concentration was significant at the shaft's shoulder chamfer, which could reduce the applied material's reliability to some extent. Meanwhile the measuring result for the radius of the shaft's shoulder chamfer showed that the actual value (2 mm) was less than the design value (5 mm), the decrease on the radius will increase the stress concentration of the shaft's shoulder chamfer, so the actual stress concentration for the shaft's shoulder chamfer was more severe than the result of the finite element simulation. Although the order torsional vibration appeared anomalous when the shaft's speed was 920 rpm, there was possible that the order torsional resonance was aroused at the relatively weak position (i.e. the site of the shaft's smallest diameter and diameter's variation) once the shaft's speed reached the critical speed's half. The synergistic effect of the high-level stress concentration and the order torsional resonance improved the failure's probability at the site of the diameter's variation, thus some microcracks would initiate during the frequency conversion conditions although the torsional fatigue strength modified of the applied material (54.15 MPa) was more twice than the calculated value (26.3 MPa) which met the requirement of design and operation. However the networked-like pearlite structure had the weak fatigue crack growth resistance [13], so the microcrack's growing was accelerated along the network structure of the grain boundary under the effect of the alternative frequency and the torsional vibration and then it led to the shaft's fracture in a short time. The typical ratchet-like fracture had provided the good evidence.

Combining with the material's mechanical properties and microstructure, it was confirm that the material's performance does not show the any evidence of aging, so the shaft's fracture was related to the high-level stress concentration and the torsional vibration which were caused by the processing and the design.

5. Conclusion

The failure of the induced draft fan's shaft in a power boiler was been investigated. The material's composition and mechanical properties satisfied the design requirement. The shaft's torsional fatigue strength revised based on the ultrasonic fatigue experiment's result confirmed the material applied was secure enough for the normal operation of the shaft. The finite element simulation based on the shaft's design size showed the stress concentration was remarkable at the shaft shoulder's chamfer (the radius was 5 mm), while the actual radius (2 mm) of the shaft shoulder's chamfer caused more significant stress concentration, so the radius the shaft shoulder's chamfer must reasonable and accurate during the process. The order torsional vibration appeared anomalous when the shaft's speed was in the critical speed. The higher stress concentration and torsional vibration induced the microcrack's initiation along the weak interface of the ferrite and the pearlite due to the network pearlite's formation; meanwhile the vibration in the induced draft fan's service led to crack growing along the different direction. The effect of the alternating torsional loading made fracture presents the typical ratchet-like characteristic.

Acknowledgement

This work was supported by Suzhou Nuclear Power Research Institute.

References

[1] He FY. Energy saving technical renovation on boiler induced draft fan using high voltage variable frequency technology. Energy Conserv Technol 2011;168:379–81.
[2] Yuan Z, Wang JB, Lin JJ, Zhang X-L, Su N, Duan H-X. High voltage frequency conversion technology application in 600 MW supercritical unit induced draft fan. J Anhui Electr Eng Prof Tech Coll 2012;3:76–9.
[3] Chen H, Sun SJ. Application and research of frequency conversion technology in 300 MW power plant induced-draft fans. Energy Conserv 2008;8:33–5.
[4] Wu WX. Application of high voltage frequency conversion technology on boiler fans for heat power plant and its effect analysis. Compres Blower Fan Technol 2008;3:65–7.
[5] Liu XC. Application of inverter on boiler wind fan. Compres Blower Fan Technol 2010;4:59–60.
[6] Joyce JS, Kulig T, Lambrecht D. Torsional fatigue of turbine-generator shafts caused by different electrical system faults and switching operations. Power Appar Syst 1978;5:1965–77.
[7] Walker DN, Adams SL, Placek RJ. Torsional vibration and fatigue of turbine-generator shafts. Power Appar Syst 1981;11:4373–80.
[8] Andrew D, George M. Torsional vibration of a shaft with a circumferential crack. Eng Fract Mech 1981;3–4:439–44.
[9] Bayraktar E, Xue H, Ayari F, Bathias C. Torsional fatigue behaviour and damage mechanisms in the very high cycle regime. Arch Mater Sci Eng 2010;2:77–86.
[10] GB.T1591-2008. High strength low alloy structural steels. Beijing: Standardization Administration of the People's Republic of China; 2008.
[11] Shi CH, Zhong QP, Li CG. China materials engineering canon. Mater Eng Found 2005;1:577–80.
[12] GB.T13299-1991. Steel-determination of microstructure. Beijing: Standardization Administration of the People's Republic of China; 1991.
[13] Korda AA, Miyashita Y, Mutoh Y, Sadasue T. Fatigue crack growth behavior in ferritic–pearlitic steels with networked and distributed pearlite structures. Int J Fatigue 2007;29:1140–8.